Supporting Information for:

Evaluating Surface Interactions in Supported Imidazolium Ionic Liquid Phases by using ultrasensitive DNP NMR and DFT studies

Hsueh-Ying Chen,[a)] Bruno B. de Araújo,[b)] Paulo F. B. Gonçalves,[b)] Gustavo Chacon Rosales,[b,c)] Francisco P. dos Santos,[b)] James Kempf,[a)] Jairton Dupont [b, d)]

[a)] Bruker BioSpin, 15 Fortune Drive, Billerica, MA 01821 USA.

[b)] Institute of Chemistry - UFRGS. Av. Bento Gonçalves, 9500, Porto Alegre, 91501-970, RS Brazil.

[c)] Instituto de Tecnología Química, Universitat Politècnica de València - Consejo Superior de Investigaciones Científicas, Av. de los Naranjos s/n, 46022 Valencia, Spain.

[d)] Departamento de Bioquímica y Biología Molecular B e Inmunología, Facultad de Química, Universidad de Murcia, E-30100 Murcia, Spain.

1. Synthesis and characterization of IL and SILP materials

The synthesis of the BEIm·Br ionic liquid was carried out as follow: a solution of fresh distilled 1-butylimidazole (0.54 g, 0.0043 mol.) and ethyl bromide (0.60 g; 0.0055 mol.) was kept in refluxing for 48 h. After this, the solution was cooled until room temperature and then all the volatiles were removed under vacuum. The resulting yellow oil solution was dissolved in a hot mixture acetone/methanol and left in fridge overnight until crystallization, filtered and dried under vacuum. The BEIm·Br ionic liquid was obtained in high yield and purity. The NMR spectra were acquired using a Varian 500 MHz spectrometer.

1-Butyl-3-ethylimidazolium bromide (BEIm·Br)

Dark orange (93%). ^{1}H NMR (CDCl3) δ (ppm): 0.67 (t, 3H, J = 7.2 Hz, $NCH_2CH_2CH2C\underline{H}_3$); 1.60 (m, 2H, $NCH_2CH_2C\underline{H}_2CH_3$); 1.33 (t, 3H, J = 7.0Hz, $NCH_2C\underline{H}_3$); 1.09 (m, 2H, $NCH_2C\underline{H}_2CH_2CH_3$); 4.10 (t, 2H, $NC\underline{H}_2CH_2CH_2CH_3$); 4.18 (q, 2H, $NC\underline{H}_2CH_3$), 7.40 and 7.54 (2s, 2H, H-5 and H-4); 10.05 (s, 1H, H-2). ^{13}C NMR δ (ppm): 13.28 ($NCH_2CH_2CH_2\underline{C}H_3$), 15.59 ($NCH_2\underline{C}H_3$), 19.23 ($NCH_2CH_2\underline{C}H_2CH_3$), 31.98 ($NCH_2\underline{C}H_2CH_2CH_3$), 45.00 ($N\underline{C}H_2CH_3$), 49.52 ($N\underline{C}H_2CH_2CH_2CH_3$), 122.15 and 122.28 (C-5 and C-4) 136.05 (C-3).

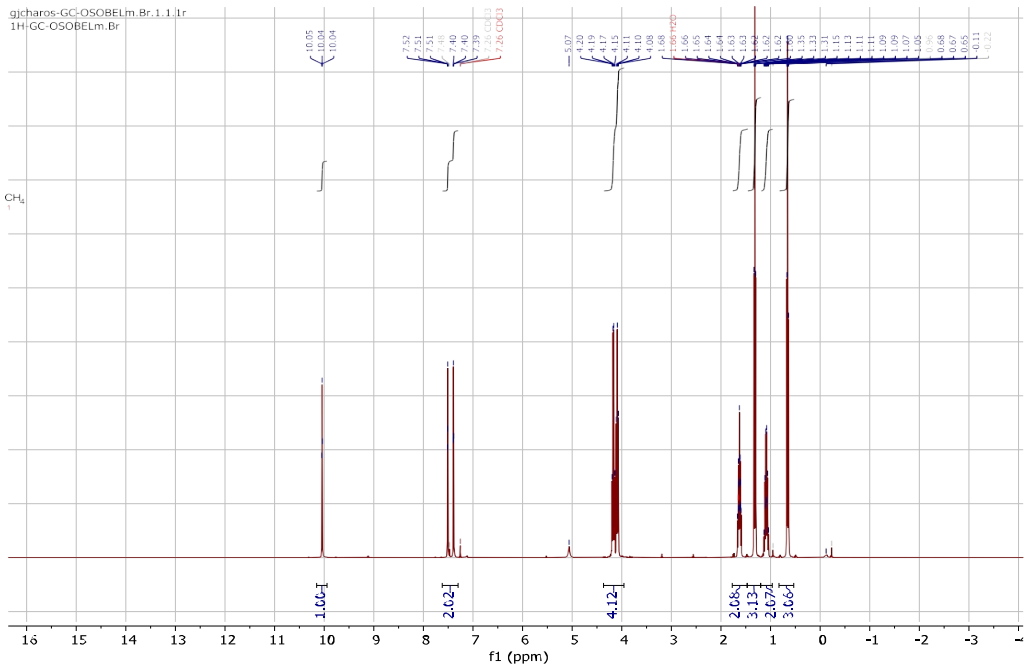

Figure S1: Solution ^{1}H NMR spectrum obtained for the ionic liquid BEIm·Br.

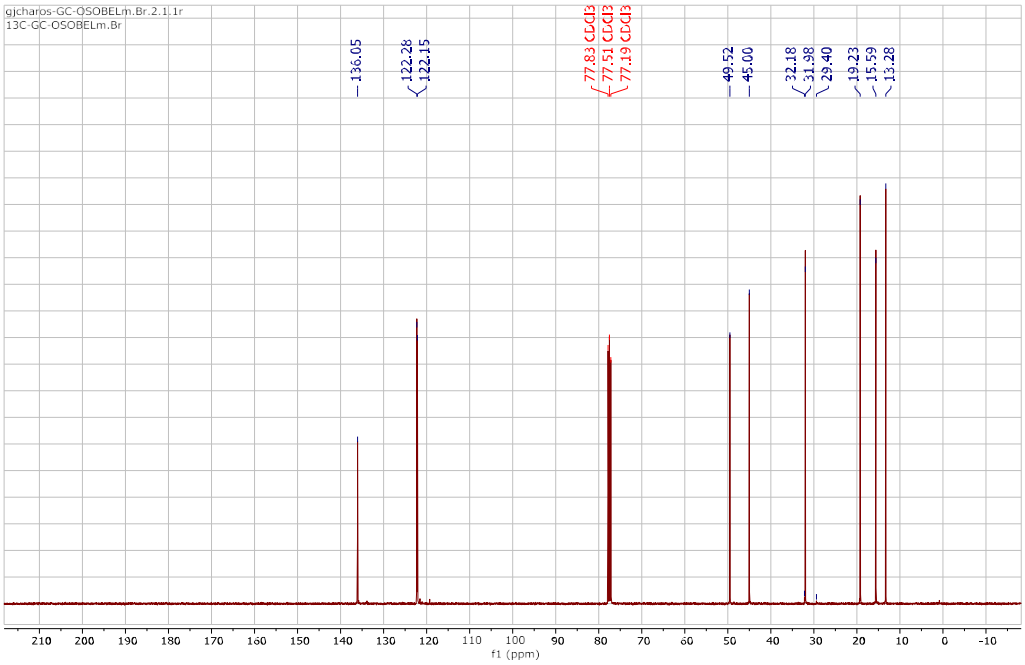

Figure S2: Solution ^{13}C NMR spectrum obtained from the ionic liquid BEIm·Br.

IL@Support (SILCA$_{BEIm·Br}$)

BEIm·Br (0.24 g; 0.0010 mol.) was dissolved in 10 mL of methanol and commercial SiO_2 (0.96 g; 0.0159 mol) was added in constant stirring during 16 h. Finally, methanol was evaporated, and the resulting white solid dried off under vacuum at 80°C for 6 h.^{13}C CP-NMR δ (ppm): 136.55 (C3), 122.61 (C4-5), 49.48 (C6), 45.80 (C2), 34.10 (C7), 19.33 (C8), 15.85 (C1), 11.54 (C9). ^{29}Si CP-NMR δ (ppm): -113.27 (s) -110.89 (s) -102.87 (s).

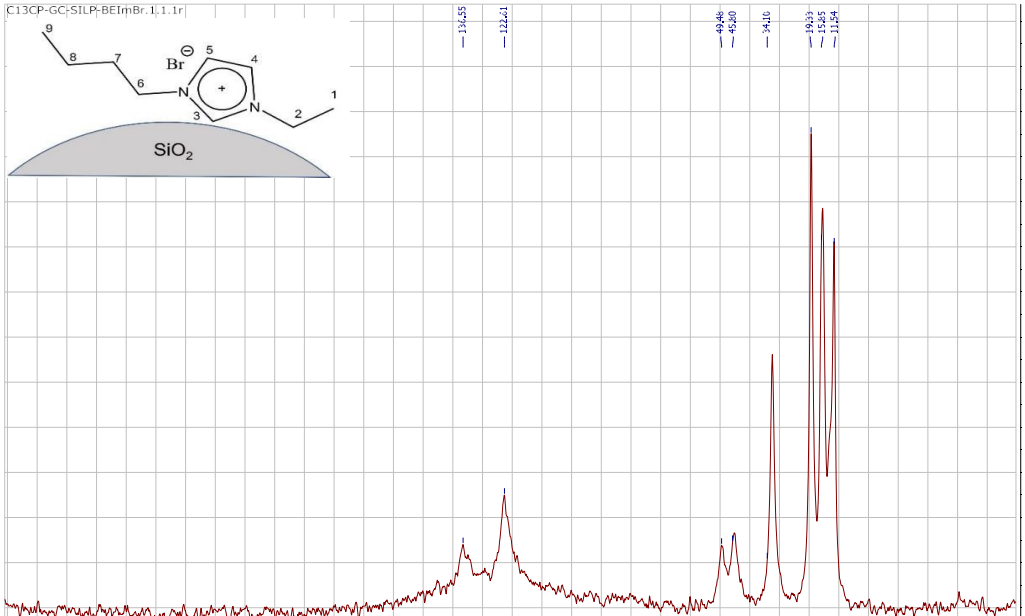

Figure S3: RT solid-state $\{^{1}H\}^{13}C$ CP-NMR spectrum obtained for *IL@Support*.

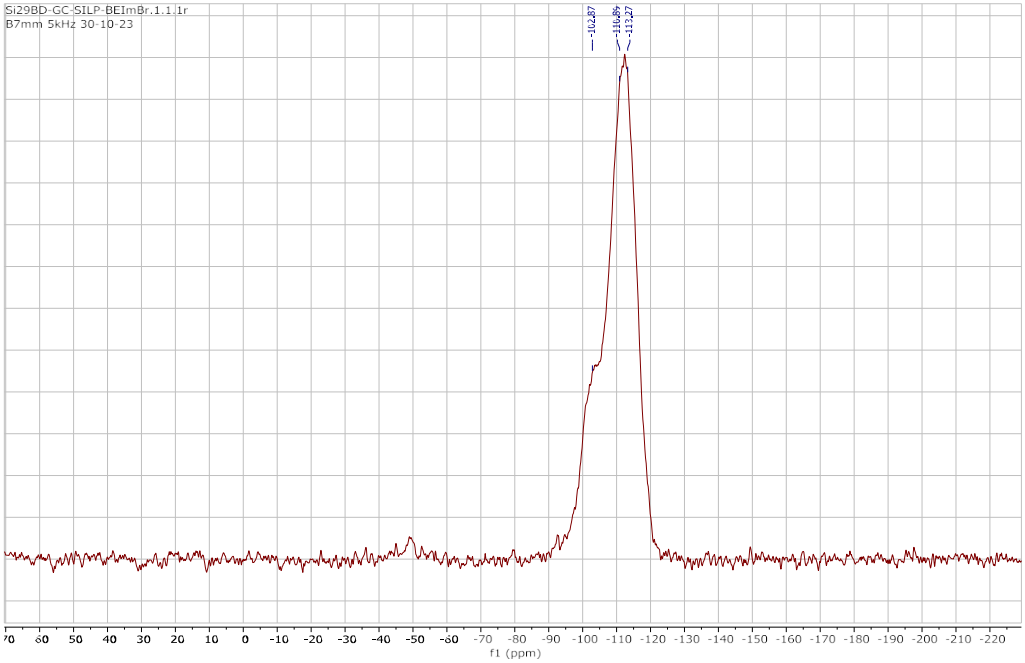

Figure S4: RT solid-state $\{^{1}H\}^{29}Si$ CP-NMR spectrum obtained for *IL@Support.*

ILG@Support (CSILP$_{EPIm\cdot Br}$)

Following a reported method,[1] activated SiO_2 (2.5 g) was suspended in fresh distilled toluene (20 mL) and (3-chloropropyl)trimethoxysilane was added drop by drop (total 2.48 g added; 0.0125 mol). This solution was refluxed for 72 h, then all the volatiles were removed under vacuum. The product chloropropyl silica gel was washed with ethanol-water-ethanol and finally dried under vacuum. This first product was dissolved with stoichiometric amounts of imidazole and refluxed during 24 h; then triethylamine was added (2 mL) and left stirring for 4h. The resulting precipitate was filtered, washed with ethyl acetate-water-ethyl acetate and dried off by vacuum for 4 h. Finally, this product was refluxed in acetone for 48 h with stoichiometric amounts of ethyl bromide, filtered and washed three times with ethyl acetate-water-ethyl acetate and, finally dried under vacuum at 60 °C for 16 h. Finally, 1-ethyl-3-(3-(trimethoxysilyl)propyl)-1*H*-imidazol-3-ium bromide, CSILP$_{EPIm\cdot Br}$ was obtained in a 95 % yield (see Scheme S1 below).

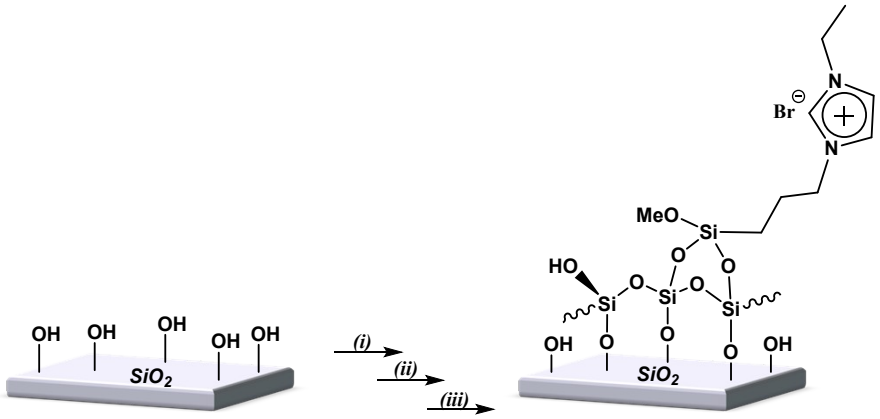

Scheme S1: Synthetic route and conditions for CSILP (*ILG@Support*) materials. (i) 3-chloropropyltrimethoxysilane, toluene, 72 h, reflux, N_2. (ii) Imidazole, toluene, 24 h, reflux, N_2, triethylamine. (iii) Ethyl bromide, acetone, room temperature, 24 hours.

Activation of SiO_2 support

Briefly, 5 g of commercial SiO_2 were embedded in 50 mL of concentrated hydrochloric acid (12 M) overnight. Then, the solid was recovered by filtration and thoroughly washed with deionized water until a neutral pH was reached. The material was then dried in a vacuum oven at 100°C overnight.

Thermogravimetric analysis (TGA)

The thermal curves for BEIm·Br, $SILCA_{BEIm·Br}$,and $CSILP_{EPIm·Br}$ are plotted in Figure S5-Figure S7 and the weight percentage of (wt%) of ionic liquid are summarized in Table S1.

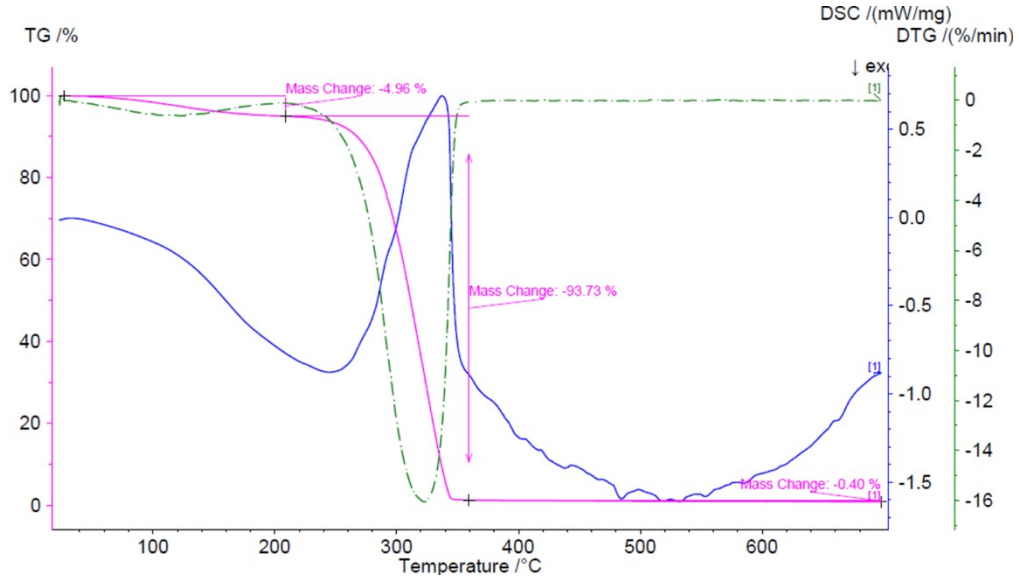

Figure S5: TG analysis report recorded for BEIm·Br ionic liquid.

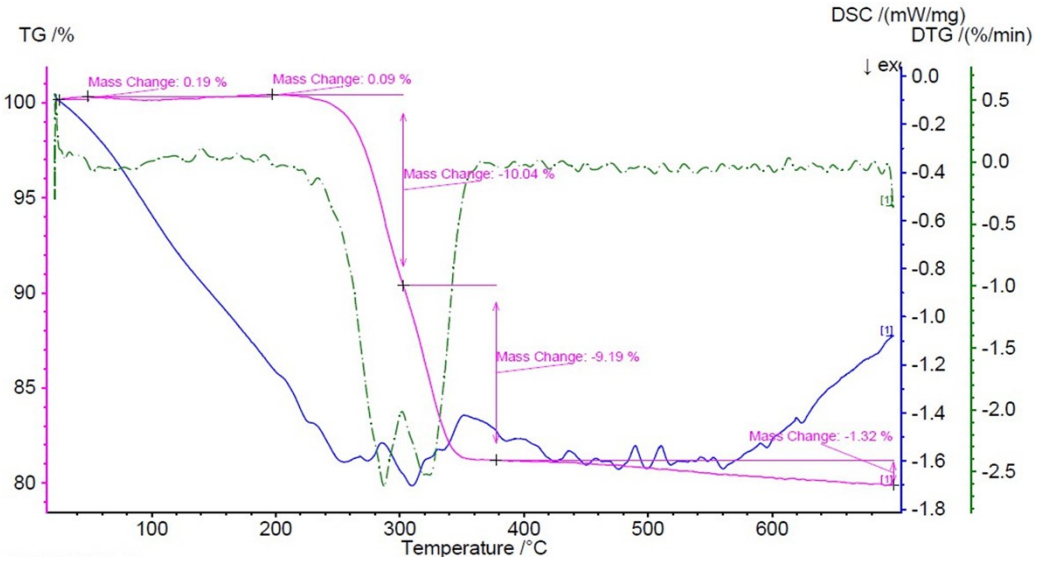

Figure S6: TG analysis recorded for *IL@Support*.

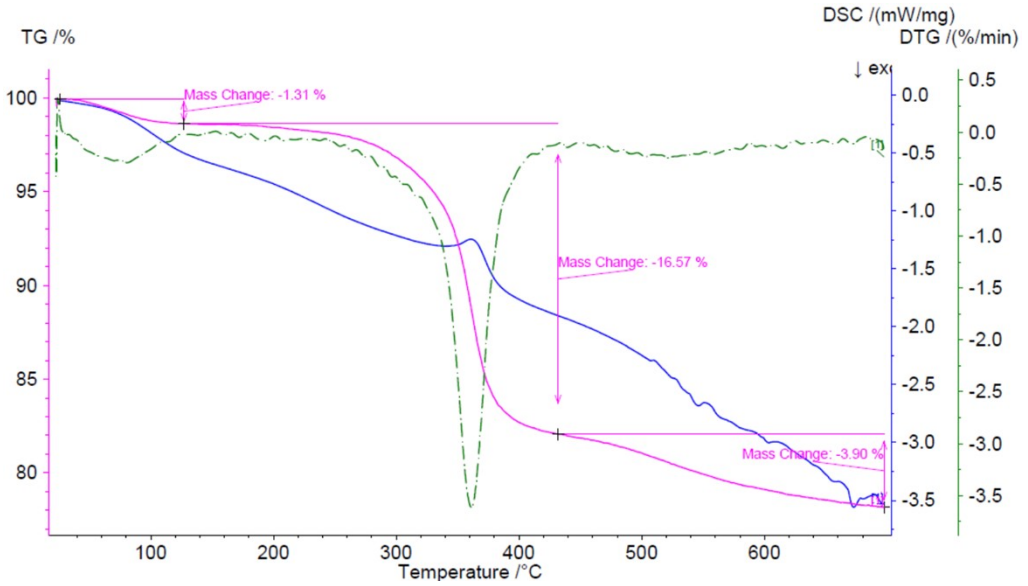

Figure S7: TG analysis recorded for *ILG@Support.*

Table S1: TGA results for ionic liquid and SILP prepared materials

IL/SILP	IL content (%)[a]	Lost water (%)	IL lost weight (%)
BEIm·Br	100.0	4.96	95.0
IL@Support **($SILCA_{BEIm·Br}$)**	20.0	0.30	19.2
ILG@Support **($CSILP_{EPIm·Br}$)**	20.0	1.31	20.5

[a] Based on the amount of ionic liquid added during preparation.

2. DNP NMR experiment

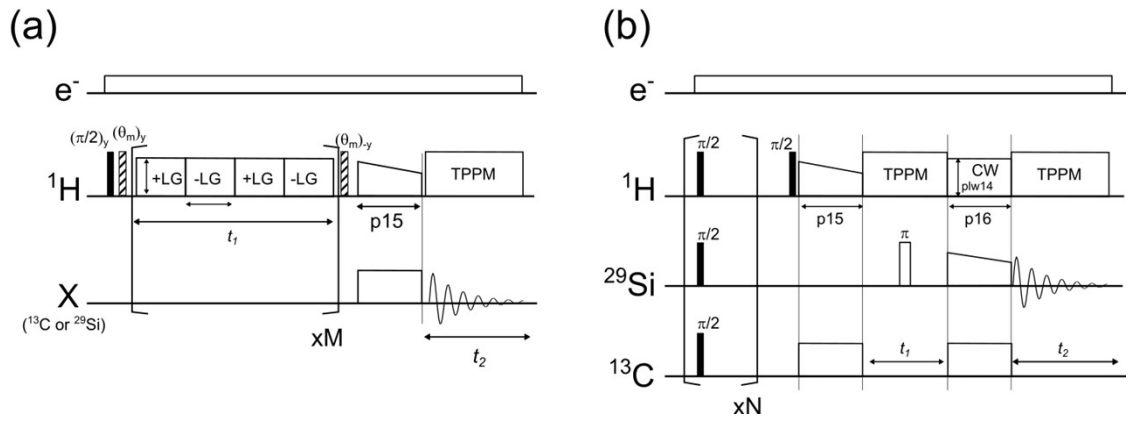

Figure S8: The 2D NMR pulse sequences used in this work (a) FSLG-HETCOR pulse sequence for ^{1}H-X correlation. The $(\theta_m)_y$ pulse refers to a 54.7° pulse with a y phase. The +LG and -LG blocks are the frequency-switched Lee-Goldburg decoupling with +x and -x phases and frequency offsets of +707 kHz and –707 kHz, respectively. (b) Double-CP based ^{13}C-^{29}Si HETCOR. The microwave was applied continuously during NMR measurements. RF field strengths and delays are shown

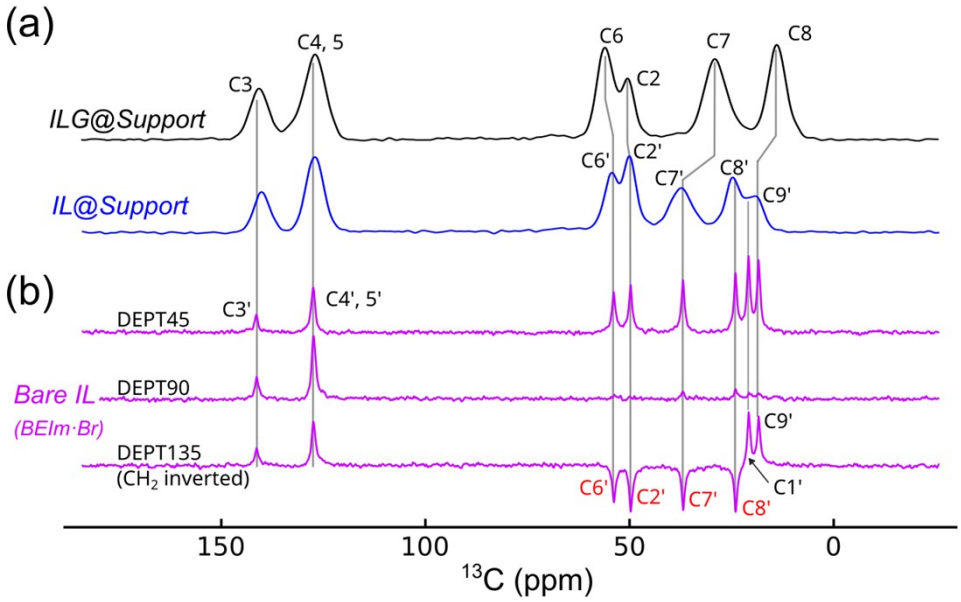

Figure S9: (a) The top two spectra are from low-temperature DNP-enhanced 1D {^{1}H}^{13}C CP experiments of *ILG@Support* and *IL@Support* samples. The bottom three room-temperature ^{13}C spectra are DEPT experiments (distortioupdatnless enhancement by polarization transfer) of bare ionic liquid as in the *IL@Support* sample.

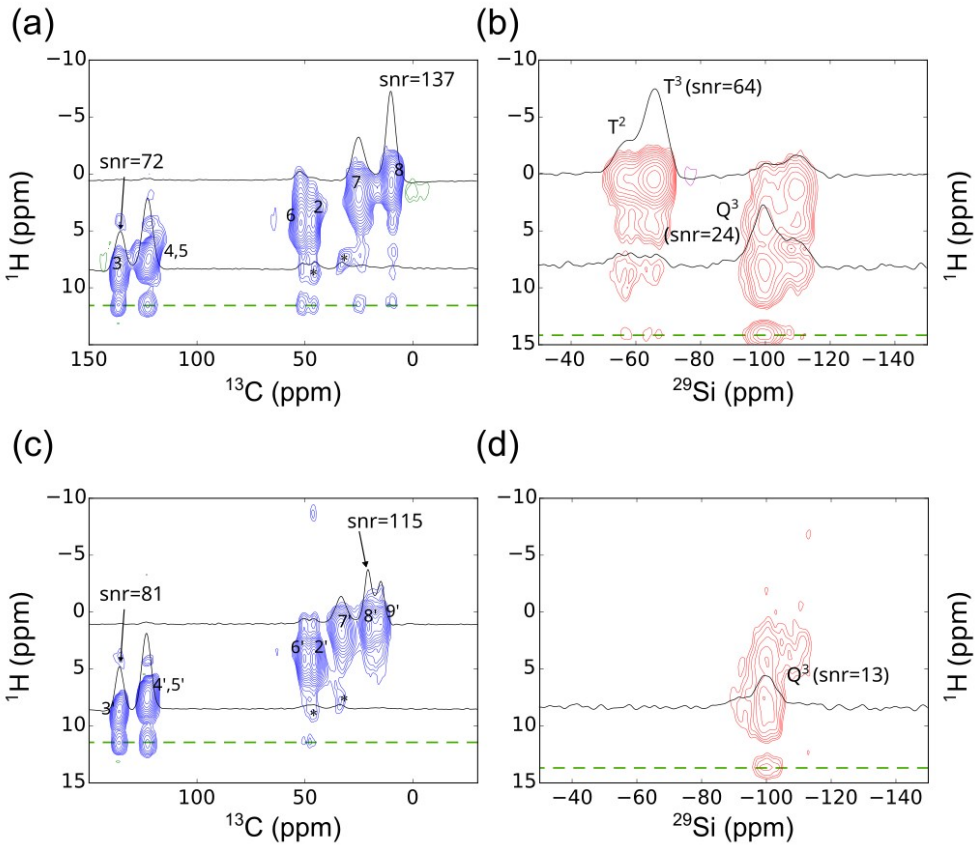

Figure S10: The same figure as the Figure 3 in the main text, again with (a,b) for grafted and (c,d) for coated samples. Here, we add representative 1D slices through ^{13}C and ^{29}Si to show the signal-to-noise. Asterisk (*) indicates spinning side bands from imidazole carbons. The center of spectral window along the indirect dimension is specified by a green dashed line where FSLG artifacts may appear.

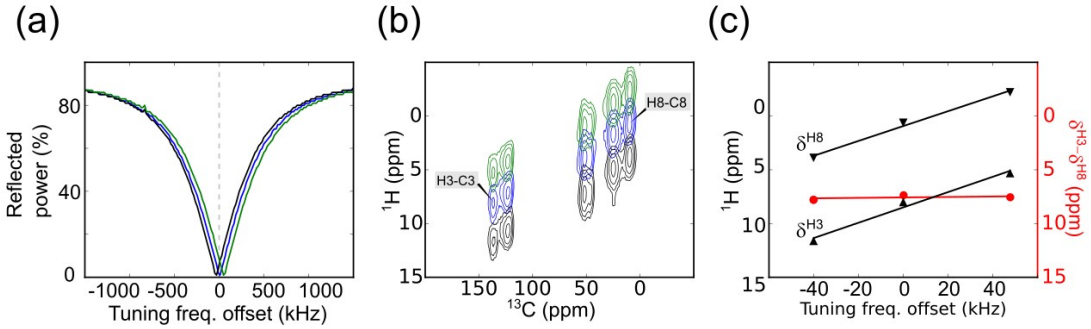

Figure S11: Impact of tuning imperfections on ^{1}H chemical-shift referencing with FSLG. (a) Intentional de-tuning of the ^{1}H channel, used to investigate the variation of the apparent ^{1}H chemical shift in the indirect dimension. The displayed instances represent variations over ±45 kHz span (~15% of FWHM of the tuning dip) (b) Corresponding ^{1}H–^{13}C FSLG-based HETCOR spectra of *ILG@Support* obtained using noted detuning. (c) Chemical shifts δ^{H3} and δ^{H8} and the difference (δ^{H3}–δ^{H3}, red) obtained with each tuning offset. The difference stays constant, indicating equivalent offset responses on the two protons. However, the apparent individual shifts respond to detuning at 0.068 ppm/kHz, emphasizing the challenge of accurate ^{1}H referencing when using FSLG.

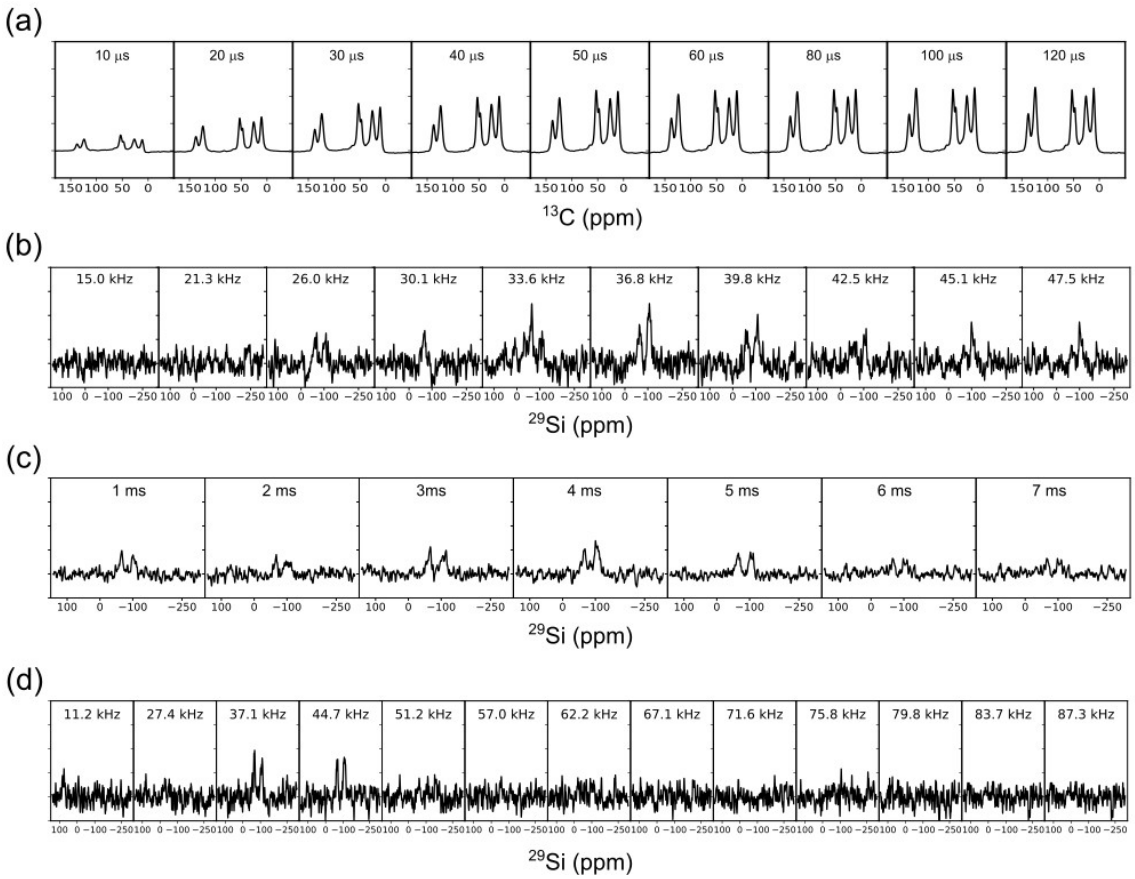

Figure S12: Parameter optimizations for ^{1}H–^{13}C–^{29}Si double CP experiment. (a) CP contact time for the first cross polarization step (^{1}H→^{13}C). (b) ^{29}Si RF field in the second CP transfer (^{13}C→^{29}Si) where ^{13}C RF field is set to 48 kHz. (c) ^{13}C→^{29}Si CP signal vs. contact time. (d) CW ^{1}H decoupling strength during (^{13}C→^{29}Si) cross polarization. In (b)-(c), each spectrum was signal-averaged for 64 scans with a recycle delay of 5s, thus requiring ~5 min for each individual 1D panel. Optimizations in (a) are much faster, using 4 scans and 5 s recycle delay, thus requiring only 20s/panel.

Table S2: Acquisition and processing parameters for solid-state NMR experiments.

Experiment	1D ^{1}H–^{13}C CP/MAS (column A)	1D ^{1}H–^{29}Si CP/MAS (column B)	2D ^{1}H–^{13}C FSLG-HETCOR	2D ^{1}H–^{29}Si FSLG-HETCOR	2D ^{13}C–^{29}Si HETCOR	2D ^{29}Si –^{13}C HETCOR
Acq. Parameters						
Number of scans	4	4	16	16	384	384
Recycle delay (s)	10	10	8	8	10	10
Spinning speed (kHz)	9	9	9	9	9	9
CP contact time (μs)	50	3000	50	200	50 ($^{1}H\rightarrow^{13}C$) 4000 ($^{13}C\rightarrow^{29}Si$)	10000 ($^{1}H\rightarrow^{29}Si$) 4000 ($^{29}Si\rightarrow^{13}C$)
CP RF field (kHz)	^{1}H: 100%-70% ramp, 57.1 kHz ^{13}C: 48.1 kHz	^{1}H:100%-70% ramp, 62.2 kHz ^{29}Si: 53.2 kHz	(same as col A)	(same as col B)	$^{1}H\rightarrow^{13}C$: (same as col A) $^{13}C\rightarrow^{29}Si$: ^{13}C: 48.1 kHz ^{29}Si: 100%-70% ramp, 37.6 kHz	$^{1}H\rightarrow^{29}Si$: (same as col B) $^{29}Si\rightarrow^{13}C$: ^{29}Si: 100%-70% ramp, 37.6 kHz ^{13}C: 48.1 kHz
Number of increments	--	--	64	64	64	64
Spectral width (Hz)	45454.5	45454.5	F2: 45454.5 F1: 28030.8	F2: 45454.5 F1: 28030.8	F2: 45457.5 F1: 35714.3	F2: 45457.5 F1: 35714.3
^{1}H decoupling during FID acq.	TPPM15 ~40 kHz	TPPM15 ~40 kHz	TPPM15 ~40 kHz	TPPM15 ~40 kHz	TPPM15 ~40 kHz	TPPM15 ~40 kHz
FSLG decoupling field strength (kHz)[1]	--	--	100.0	100.0		
Proc. parameters						
Apodization	GM LB = - 200 Hz, GB = 0.1	GM LB = - 200 Hz, GB = 0.1	GM F2: LB = -200 Hz, GB =0.1 F1: LB = -200 Hz, GB = 0.5	GM F2: LB = -200 Hz, GB = 0.1 F1: LB = -200 Hz, GB = 0.5	F2 (EM): LB = 200 Hz F1(GM) LB = -200 Hz, GB = 0.3	F2 (EM): LB = 200 Hz F1(GM) LB = -200 Hz, GB = 0.3

[1] frequency offset calculated automatically in standard Bruker pulse sequence.

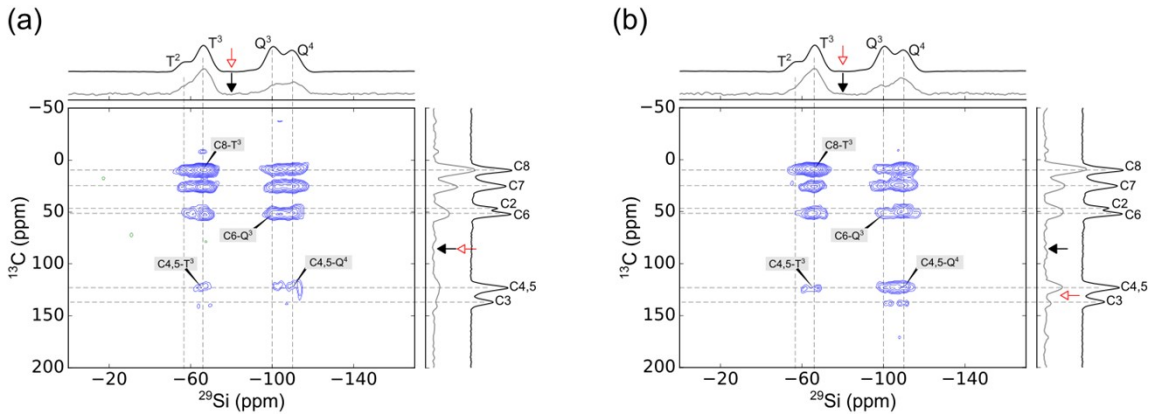

Figure S13: Explore the effect of RF carriers for $^{1}H–^{13}C–^{29}Si$ double CP experiment. Hollow red arrows refer to ^{13}C and ^{29}Si RF carriers during $^{13}C–^{29}Si$ CP transfer step. Solid black arrows refer to detection carrier frequency. Adjacent 1D panels at the top and at the right overlay projections from the 2D (gray) with 1D CP spectra (black) from Figure 2 in the main text.

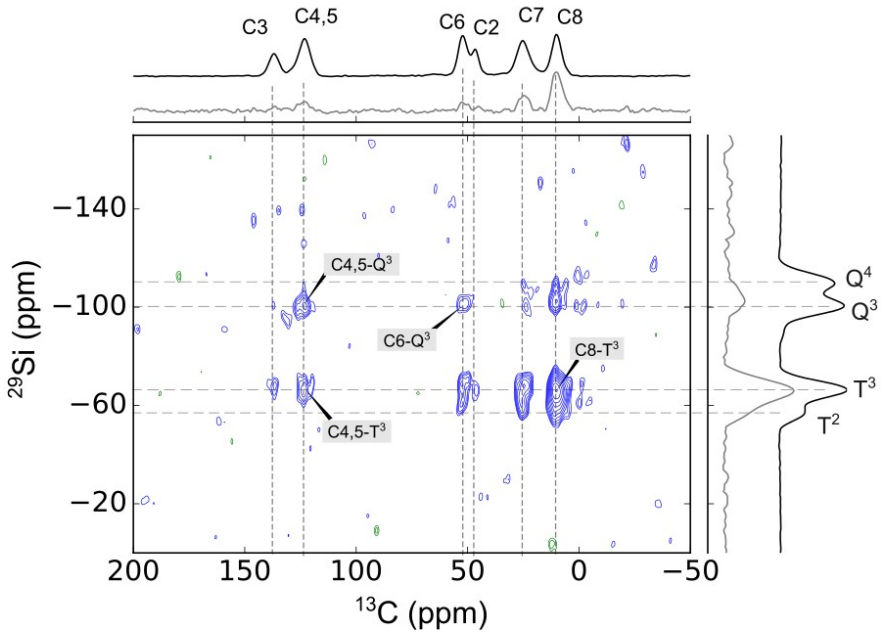

Figure S14: Spectra with alternative ordering $^{1}H–^{29}Si-^{13}C$ of double CP transfers, thus providing higher-resolution direct detection for ^{13}C.

DFT studies

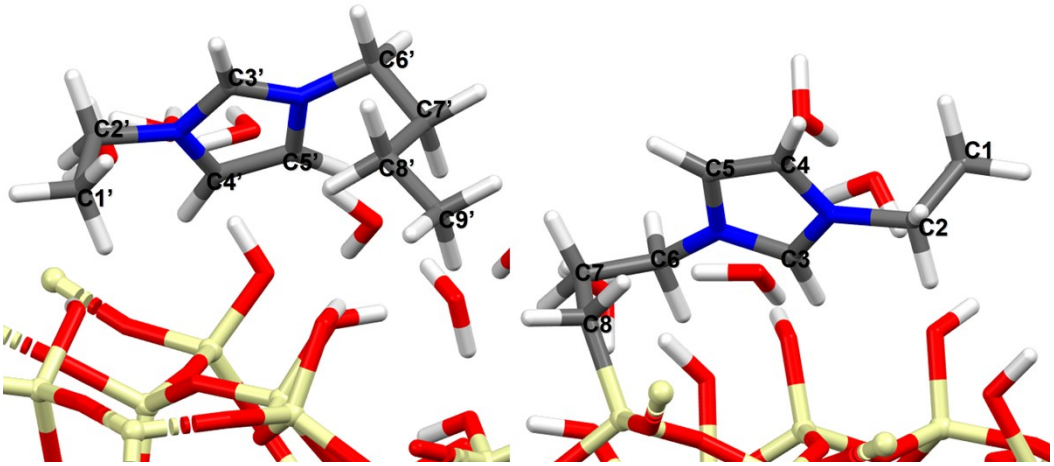

Figure S15: Interaction distances involved in *IL@Support* and *ILG@Support* surface calculated by DFT

Table S3: The distance of nitrogen and carbon atoms to the nearest silica surface sites in Angstrom. The notation "( )" refers to the averaged distance of included atoms.

IL@Support 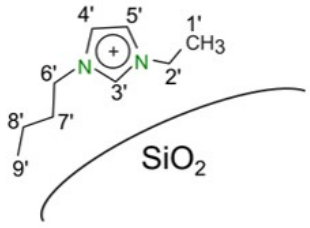		*ILG@Support* 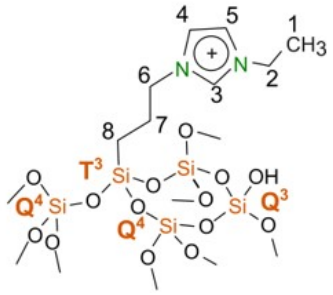	
N – T3	**N.A.**	**N – T3**	**4.5**
N – Q3	**5.4**	**N – Q3**	**3.9**
N – Q4	**6.2**	**N – Q4**	**4.6**
(C1', C2') – Q3	**4.3**	**(C1, C2) – Q3**	**5.4**
(C1', C2') – Q4	**4.9**	**(C1, C2) – Q4**	**5.7**
(C6', C7', C8', C9') – Q3	**5.5**	**(C6, C7, C8) – Q3**	**5.0**
(C6', C7', C8', C9') – Q4	**6.2**	**(C6, C7, C8) – Q4**	**4.7**
		C6 – T3	**3.6**
		C6 – Q3	**4.3**
		C6 – Q4	**4.5**
		C2 – T3	**6.1**
		C2 – Q3	**5.2**
		C2 – Q4	**5.1**

Table S4: Distance between hydrogen atoms and Si-T^3, in *ILG@Support* case, and Si-Q^3 and Si-Q^4, in IL@Support case, in Angstrom.

	Si-T^3 ***of ILG@Support***		**Si-Q^3/Q^4** ***of IL@Support***
C1 ($-CH_3$)	8.2	**C1'** ($-CH_3$)	5.0/4.6
	7.8		4.1/4.6
	7.4		3.3/3.3
C2 ($-CH_2-$)	6.4	**C2'** ($-CH_2-$)	5.5/6.4
	5.8		3.9/5.5
C3 (–CH–)	4.4	**C3'** (–CH–)	6.5/6.8
C4 (–CH–)	6.0	**C4'** (–CH–)	3.7/4.5
C5 (–CH–)	4.8	**C5'** (–CH–)	4.2/6.8
C6 ($-CH_2-$)	4.6	**C6'** ($-CH_2-$)	7.0/8.2
	3.3		6.8/8.6
C7 ($-CH_2-$)	3.9	**C7'** ($-CH_2-$)	6.5/8.3
	3.2		4.9/7.1
C8 ($-CH_2-$)	2.4	**C8'** ($-CH_2-$)	6.1/7.0
	2.4		4.3/5.4
		C9' ($-CH_3$)	4.8/7.7
			4.1/6.2
			3.8/6.2

3. References

[1] O. Martínez-Ferraté, G. Chacón, F. Bernardi, T. Grehl, P. Brüner, J. Dupont, *Catal. Sci. Technol.* **2018**, *8*, 3081-3089.